

Biotransmutation as a Cold Fusion Phenomenon*

Hideo Kozima,

Cold Fusion Research Laboratory <http://www.geocities.jp/hjrfq930/>

597-16 Yatsu, Aoi, Shizuoka, 421-1202 Japan

Abstract

The nuclear transmutations in biological systems (biotransmutations) have been investigated for more than two centuries as reviewed in several books by Komaki and Kush and we have analyzed them tentatively by using our TNCF model developed for the cold fusion phenomenon (CFP) in transition metal hydrides/deuterides. Recently, the investigation of the biotransmutations made a great progress in the direction to determine the microscopic origin of the nuclear reactions in the biological system where is apparently no mechanism to accelerate charged particles up to enough energies to cause fusion reactions of nucleons. Vysotskii et al. have shown not only the biotransmutation but also the decay-time shortening of radioactive nuclides in systems including microbial cultures: There are data sets showing (1) production of $^{57}_{26}\text{Fe}$ from $^{55}_{25}\text{Mn}$ and also (2) acceleration of the decay of radioactive nucleus $^{137}_{55}\text{Cs}$, $^{140}_{56}\text{Ba}$ and $^{140}_{57}\text{La}$ in several bacterial cultures. In this paper, we have reexamined the data of biotransmutation and decay-time shortening of radioactive nuclides in microbial cultures from molecular levels and applied our TNCF model to analyze them. It is shown that the TNCF model successful to give a unified explanation of the CFP is applicable also to the biotransmutation.

1. Introduction

In the events of the cold fusion phenomenon (CFP), the nuclear transmutation (NT) is an astonishing one from the viewpoint of nuclear physicists suggesting a new state of matter in the CF materials (materials responsible to the CFP) entirely different from the states of matter we know in physics and chemistry developed in the 20th century.

It is remarkable to notice that the nuclear transmutations in biological systems (biotransmutations) have been investigated for more than two centuries as reviewed in several books [Komaki 1993, Kushi 1994] before the discovery of the CFP in chemical systems in 1989. We have analyzed tentatively these historical data by our phenomenological model [Kozima 1996].

Recently, the investigation of the biotransmutations made a great progress in the direction to determine the microscopic origin of the nuclear reactions in the biological

systems where is apparently no mechanism to accelerate charged particles up to enough energies to cause fusion reactions of nucleons in the meaning of usual nuclear physics. Vysotskii et al. [Vysotskii 2009a] have shown not only the biotransmutation but also the decay-time shortening of radioactive nuclides in systems including microbial cultures: There are data sets showing (1) production of $^{57}_{26}\text{Fe}$ from $^{55}_{25}\text{Mn}$ and also (2) acceleration of the decay of radioactive nucleus $^{137}_{55}\text{Cs}$, $^{140}_{56}\text{Ba}$ and $^{140}_{57}\text{La}$ in several bacterial cultures. To solve the riddle of nuclear reactions occurring in biological systems, the TNCF model [Kozima 1998, 2006] was applied to them which had been applied successfully to various events in the cold fusion phenomenon (CFP) in chemical systems [Kozima 2015].

About the CFP general, we have given reviews of typical experimental data sets and their explanations based on our model [Kozima 1998 (Chapter 9), 2006 (Section 2.5), 2014a]. An extensive bibliography of the data in the CFP was also given by Storms in his book [Storms 2007 (Section 4.5)].

In the successful explanation of the CFP by the TNCF model, the most remarkable discovery is the stability law for the frequency of detection of a transmuted nucleus in the CFP comparing the experimental data with the abundance of elements in universe [Kozima 2005, 2006 (Section 2.11), Suess 1956]. The stability law for the transmuted nuclei in the CFP suggests that the mechanism working in the CF materials (materials where observed the CFP) should be similar to the mechanism of elements production in the universe.

To approach the real mechanism resulting in the CFP, we have investigated quantum mechanically the premises of the TNCF model, especially the existence of neutrons (trapped neutrons) in the CF materials. The characteristics of the trapped neutrons participating in the CFP are revealed by its wave nature with their de Broglie wave length λ_D comparable to the lattice constants of the CF materials [Kozima 1994]. The neutron with an energy E as an elementary particle exhibits wave property with a characteristic wave length λ_D (called de Broglie wave length)

$$\lambda_D = h/p = h/(\sqrt{2m_n E}), \quad (1.1)$$

where m_n is the neutron mass and h is the Planck's constant. The de Broglie wave length takes a value

$$\lambda_D = 1 \times 10^{-8} \text{ cm} = 0.1 \text{ nm} = 100 \text{ pm} \quad (E = 98 \text{ meV} = 0.098 \text{ eV})$$

for a kinetic energy of $E = 0.098 \text{ eV}$, and

$$\lambda_D = 1.80 \times 10^{-8} \text{ cm} = 1.80 \text{ \AA} = 0.18 \text{ nm} = 180 \text{ pm} \quad (E = E_{\text{th}} \equiv 25 \text{ meV})$$

for $E = E_{\text{th}} \equiv 25 \text{ meV} = 0.025 \text{ eV}$ (the thermal energy at 300 K).

([Kozima 1998 (Section 12.2c)])

The relation (1.1) is plotted in Fig. 1.1. As we see in the diagram, the de Broglie wave length of a neutron decreases with the inverse-square-root of energy; the wave length of 180 pm at $E = 25$ meV increases to 360 pm at $E = (25/4)$ meV = 6.25 meV. As we see in the following sections and Appendix 1, almost all the lattice constants of CF materials including biological systems are in the range between this two values, 180 pm and 360 pm (cf. especially Figs. A3 – A5 in Appendix 1).

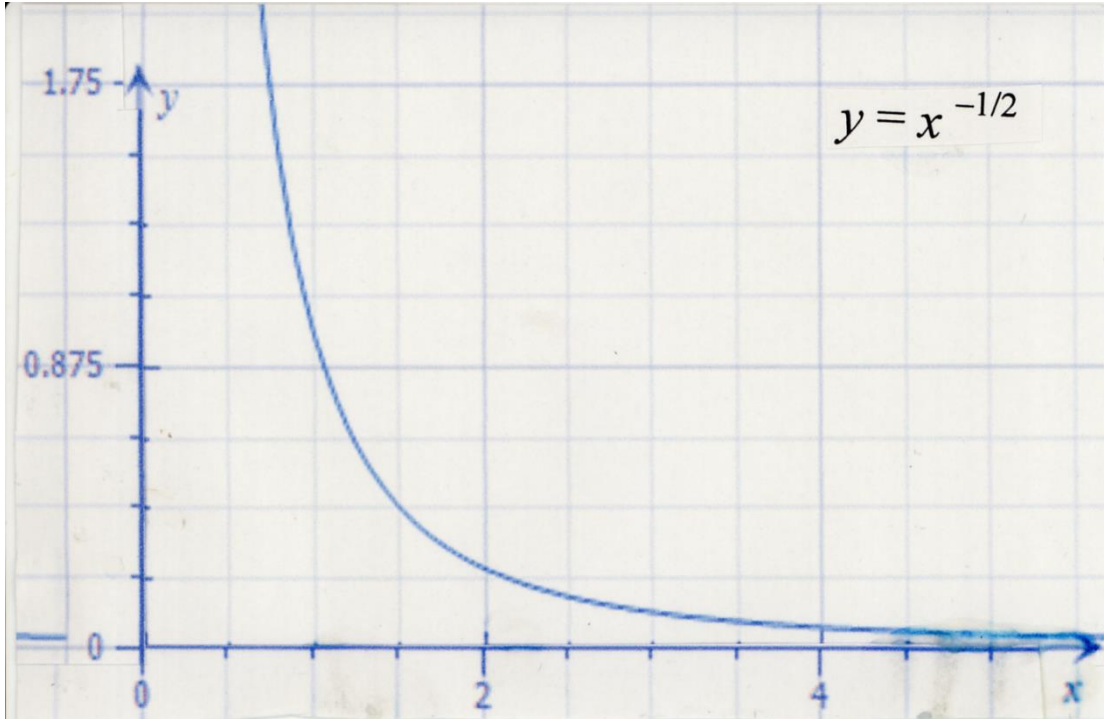


Fig. 1.1 Diagram of $x (= 2m_n E/h^2)$ vs. $y (= \lambda_D)$. Neutron energy $E = 25$ meV corresponds to the wave length $\lambda_D = 180$ pm. The more the neutron energy decreases, the more the de Broglie wave length lengthens.

It is helpful to recollect nuclear transmutations in transition-metal hydrides which were recently reviewed in our paper [Kozima 2014b]. We show the crystal structure of NiH, one of typical CF materials in transition-metal hydrides, in Fig. 1.2. The lattice constant a of NiH is $3.731 \text{ \AA} = 373.1$ pm.

As was explained generally in our recent papers [Kozima 2014a, 2016a], a neutron in a lattice nucleus Ni interacts with another neutron in another lattice nucleus Ni mediated by interstitial protons at nearest sites of the both Ni (the super-nuclear interaction). Then as a result of this super-nuclear interaction between lattice nuclei, there appear neutron bands where are neutrons participating in the nuclear reactions in the CFP.

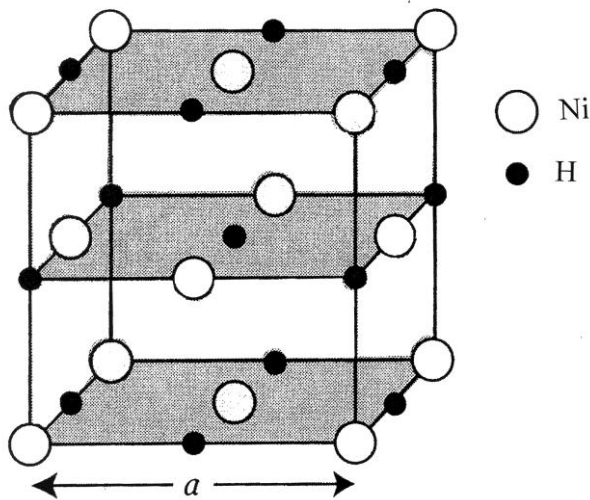


Fig. 1.2 Atomic arrangement in nickel hydride crystal. Ni(\circ) atoms locate at corners and centers of faces of a cube with an edge of length a . Hydrogens (\bullet) locate at octahedral interstices (interstitial sites) surrounded by six Ni atoms in this case. (Another interstices surrounded by four Ni atoms are called tetrahedral sites.) The lattice constant a is $3.731 \text{ \AA} = 373.1 \text{ pm}$.

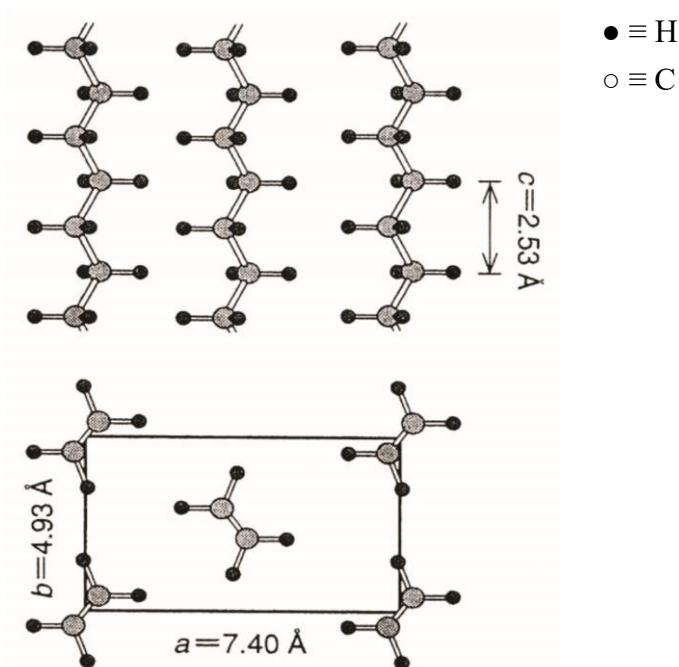


Fig. 1.3 Lattice structure of XLPE orthorhombic lattice with lattice constants, $a = 7.40 \text{ \AA}$ (740 pm), $b = 4.93 \text{ \AA}$ (493 pm), $c = 2.53 \text{ \AA}$ (253 pm) [Kozima 2010 (Fig. 5)].

Similarly, we can contemplate appearance of neutron bands in XLPE shown in Fig. 1.3 [Kozima 2010]. The rather regular structure of the carbon-hydrogen array in XLPE

suggests similar mechanism to form the neutron bands as discussed in our recent paper [Kozima 2010, 2016b]. The atomic arrays in biological cells are more complex compared with that in XLPE as seen in the following pages and Appendix but we may be able to use the same idea used in the CFP general in biological systems.

2. Biotransmutation

There is a long history of observations of curious events, nuclear transmutations in biological systems, i.e. biotransmutations [Komaki 1993, Kushi 1994]. These events have been out of a scope of modern science especially because there was lack of microscopic evidences for the events. Recent investigation of the biotransmutation supplied microscopic knowledge of the systems in which occur the events.

We give a historical review on the biotransmutation in the first subsection and introduce new data sets obtained by Vysotskii et al. in the next subsection.

2.1 Historical Review of Nuclear Transmutations in Biological Systems

Biotransmutation had been noticed very long ago in 1799 by Vauquelin as described by M. Kushi [Kushi 1994].

“A belief in the possibility of transmutation dates back to the origin of modern science. In 1799, a French chemist by the name of Vauquelin observed a large quantity of lime (CaO) in the daily excretion of chickens. He fed a captive hen a diet of nothing but oats in order to find out where the lime was coming from. He measured the amount of lime in the oats, and then fed the oats to the hen. He then measured the amount of lime in the excretion and the eggs of the hen, and discovered that it had increased by a factor of twelve. He hypothesized that lime had been created but was unable to explain how or why.” [Kushi 1994, Kozima 1998 (Section 10.1)]

A possible explanation of the biotransmutation known by the year of 1998 was given in our old book [Kozima 1998 (Section 10.1)]. From the developed point of view of the TNCF model, we have to revise the explanation given there as follows.

The expression given there;

“It might be not absurd if we consider that a living being create a structure feasible to trap thermal neutrons when necessity be felt to transmute potassium into sodium, or else.” (underlined at citation),

should be rewritten as follows,

“It might be not absurd if we consider that a living being create a structure feasible to trap thermal neutrons or to form the neutron bands through the super-nuclear”

interaction between lattice nuclei mediated by protons at interstitials when necessity be felt to transmute potassium into sodium, or else.”

The experimental investigation of the biotransmutation has made vast progress in these more than ten years and we can give a more quantitative treatment using developed knowledge of the mechanism of the CFP.

2.2 Recent Experimental data sets by Vysotskii et al.

The experimental data sets in biological systems have been obtained in these about 20 years mainly by V.I. Vysotskii and his collaborators [Vysotskii 1996, 2000, 2009a, 2009b, 2013, 2015a, 2015b]. To realize the complex structure of bacteria and microbial cultures used in their experiments, we give their fundamental structures in Appendix 1. The figures depicted in Appendix 1 show complex but similar regular structures in microbial cultures to that in XLPE shown in Fig. 1.3.

There are data sets showing (1) production of $^{57}_{26}\text{Fe}$ from $^{55}_{25}\text{Mn}$ and also (2) acceleration of the decay of radioactive nucleus $^{157}_{55}\text{Cs}$, $^{140}_{56}\text{Ba}$ and $^{140}_{57}\text{La}$ in several bacterial cultures.

Experiments were conducted using several bacterial cultures (*Bacillus subtilis* GSY 228, *Escherichia coli* K-1, *Deinococcus radiodurans* M-1) as well as the yeast culture *Saccharomyces cerevisiae* T-8. Selection of these cultures was motivated either by their experimentally proven ability to grow in the heavy water based media or by the prospect of using the radiation-stable culture *Deinococcus radiodurans* M-1 in transmutation processes given the presence of powerful radioactive fields, as was noted earlier [Vysotskii 2009a].

The bacterial cultures used in their experiments have following characteristics:

***S. cerevisiae* (*Saccharomyces cerevisiae*)** cells are round to ovoid (egg shaped), 5–10 micrometers (μm) in diameter.

***B. subtilis* (*Bacillus subtilis*)** cells are typically rod-shaped, and are about 4-10 μm long and 0.25–1.0 μm in diameter, with a cell volume of about 4.6 fL at stationary phase.

***D. radiodurans* (*Deinococcus radiodurans*)** is a rather large, spherical bacterium, with a diameter of 1.5 to 3.5 μm . Four cells normally stick together, forming a tetrad.

***E. coli* (*Escherichia coli*)** is - - - . Cells are typically rod-shaped, and are about 2.0 μm long and 0.25–1.0 μm in diameter, with a cell volume of 0.6–0.7 μm^3 .

The observed acceleration of the decay process of $^{137}_{55}\text{Cs}$ isotope is shown in

Fig. 2.1. The behavior of the decay time shortening in transition-metal hydrides had been noticed before and discussed in our paper already [Kozima 2014c].

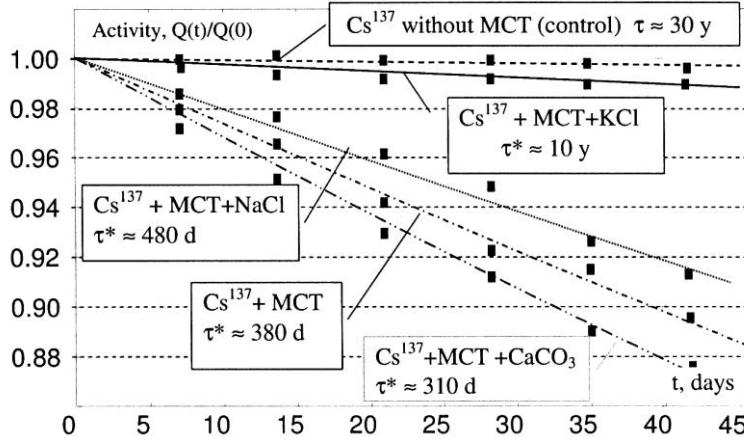


Fig. 2.1 Accelerated deactivation (accelerated decay) of $^{137}_{55}\text{Cs}$ isotope in “biological cells” with presents of different chemical elements [Vysotskii 2009a (Fig. 3.23), 2013 (Fig. 10)]. “MCT” in the explanation of this figure means the microbial catalyst-transmutator, a special kind of granules. (Cf. Appendix 2 of this paper).

Another data of the decay-time shortening in the biological system is obtained in $^{140}_{56}\text{Ba}$ and $^{140}_{57}\text{La}$ in pure reactor water with presence of metabolically active microorganisms as shown in Fig. 2.2.

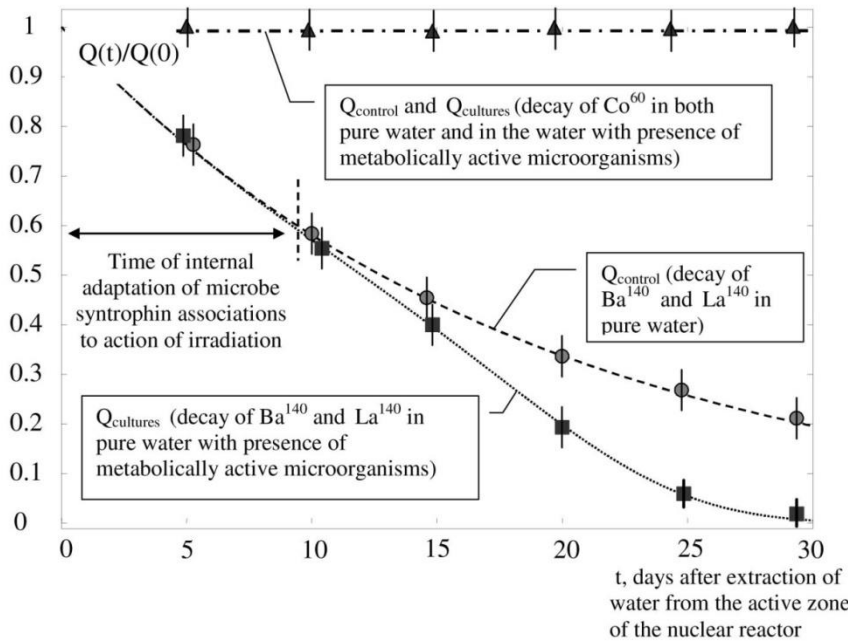


Fig. 2.2 Change of activity $Q(t)$ of the same reactor $^{140}_{56}\text{Ba}$, $^{140}_{57}\text{La}$ and $^{60}_{27}\text{Co}$ isotopes in the experiment on transmutation (activity Q_{cultures} in pure reactor water with presence

of metabolically active microorganisms) and in the control one (activity Q_{control} in the same pure reactor water without microorganisms) [Vysotskii 2009a (Fig. 3.21), 2013 (Fig. 8)].

We can show the molecular structure of the *Escherichia coli* ribosome in Fig. 2.3 used in the experiments by Vysotskii et al. (e.g. [Vysotskii 2009a]).

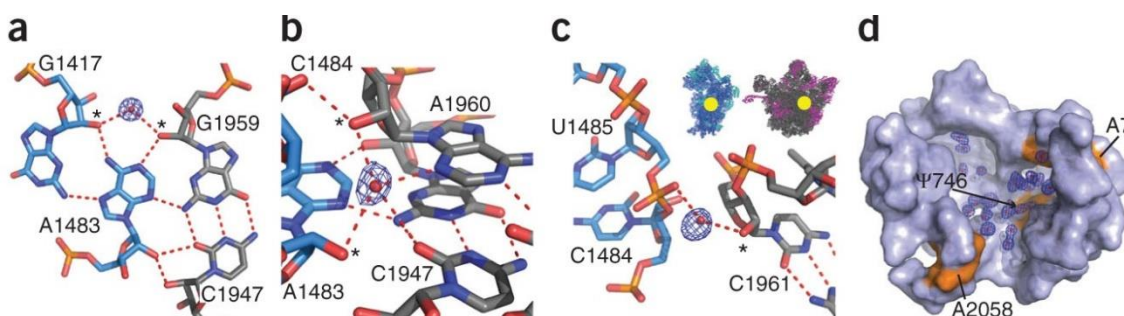


Fig. 2.3 *Escherichia coli* ribosome [Noeske 2015]

3. Theoretical Investigation on the Biotransmutation in Bacterial Cultures

The structures of bacterial cultures used in the experiments by Vysotskii et al. [Vysotskii 1996, 2000, 2009a, 2009b, 2013] are too complicated to treat them in a parallel way to the cases of transition-metal hydrides [Kozima 2014a] and XLPE [Kozima 2012]. We can, however, give explanations of the nuclear transmutations of $^{55}_{25}\text{Mn}$ into $^{57}_{26}\text{Fe}$ and the decay-time shortening of $^{137}_{55}\text{Cs}$, $^{140}_{56}\text{Ba}$ and $^{140}_{57}\text{La}$ (and invariance of τ in the case of $^{60}_{27}\text{Co}$) on a qualitative justification of application of the TNCF model to these cases.

First of all, we have to recognize the characteristics of bacteria in relation to the interaction with thermal neutrons. The distances between nuclei appropriate to effective interaction with thermal neutrons and regular arrangements of molecules in hydrocarbons in components of bacteria are two important characteristics common to the cultures used by Vysotskii et al. for the nuclear transmutation. These characteristics remind us the words cited by M. Kushi in his book [Kushi 1994 (p. 25)] from a report, *Energy Development from Elemental Transmutations in Biological Systems*, published by U.S. Army Material Technology Laboratory in 1978;

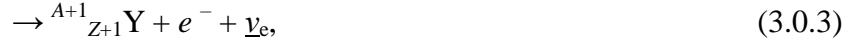
“The MgATP when place in layers one atop the other has all the attributes of a cyclotron in accordance with the requirements set forth by E.O. Lawrence, inventor of the cyclotron” [Kozima 1998 (Section 10.1)]. A possibility of nuclear reactions in biological cells had been recognized to explain the NTs observed by the year of 1978 as

the sentence cited above shows.

Allowing application of the TNCF model to the problems of biotransmutation, we can use following reactions between a trapped neutron n and a nucleus ${}^A_Z\text{X}$ at or in the surface of a bacterium;



In this reaction formula, ${}^{A+1}_Z\text{X}^*$ is an excited state of the nucleus ${}^{A+1}_Z\text{X}$ which will decay through following several channels in free space;



where $\underline{\nu}_e$ is an electron neutrino, γ is a photon (in free space) and Y, Y' and Y'' are daughter nuclides of the reactions. In the CF materials, the photon γ in the free space is supposed to be absorbed by the cf-matter formed of neutrons in the neutron band and its energy dissipates in phonons to heat the system as a whole [Kozima 2006 (Section 3.7.5)].

We would like to add another possibility to the dissipation mechanism resulting in the decay-time shortening in addition to the above mechanism proposed before [Kozima 2014c]. The decay process of a radioactive nuclide ${}^{A+1}_Z\text{X}$ to another ${}^A_Z\text{Y}$ may be strongly influenced by the interaction with a thermal neutron. The possible influence of the thermal neutron is described as (3.0.7) in the case of a beta-decay (3.0.6) in free space;



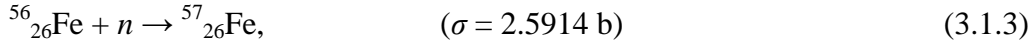
Therefore, we have two possible effects of the trapped neutrons (3.0.1) and (3.0.7) on the decay process of radioactive nuclides.

3.1 Explanation of Nuclear Transmutations in Biological System (Biotransmutation)

Now, let us investigate the biotransmutation observed by Vysotskii et al.

The first example is the production of ${}^{57}_{26}\text{Fe}$ in a CF material containing ${}^{55}_{25}\text{Mn}$. The nuclear reaction responsible to this case is suggested by Eqs. (3.0.3) and (3.0.2). We can explain the production of ${}^{57}_{26}\text{Fe}$ from ${}^{55}_{25}\text{Mn}$ by the following reactions based on the TNCF model;





3.2 Explanation of Decay-Time Shortening in Biological System

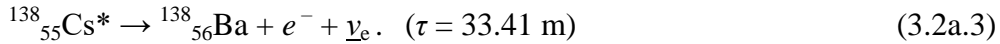
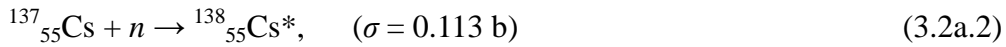
The sophisticated experiments performed by Vysotskii et al. on the nuclear processes in biological systems revealed existence of the decay-time shortening observed already in inorganic CF systems as discussed recently in our paper [Kozima 2014c]. There are two examples of the decay-time shortening in biological system; one for ${}^{37}_{55}\text{Cs}$ in electrolytic liquid, MCT + electrolyte (KCl, NaCl, or CaCO_3), and another for ${}^{140}_{56}\text{Ba}$ and ${}^{140}_{57}\text{La}$ in electrolytic liquid (water + metabolically active microorganisms). Explanation of MCT used in the experiment is given in Appendix 2.

3.2a ${}^{37}_{55}\text{Cs}$

The second example is the decay time shortening of radioactive isotope ${}^{137}_{55}\text{Cs}$ which decays in free space according to the following reaction shown in Fig. 2.1;



Assuming the existence of the trapped neutron in the TNCF model, we can apply the equation (3.0.3) to this case;



The difference of the effect of MCT (microbial catalyst-transmutator) + electrolyte (KCl, NaCl, or CaCO_3) on the decay-time shortening may express (1) difference of the density of the trapped neutrons n_n or (2) difference of the number of ${}^{137}_{55}\text{Cs}$ nuclei on the MCT surface in the system due to the effect of electrolytic liquids (MCT + electrolytes) on the MCT.

The measured decay times $\tau^* = 380 \text{ d}$ (MCT), 10 y (MCT + KCl), 480 d (MCT + NaCl), and 310 d (MCT + CaCO_3) compared to the natural decay time 30.1 y of ${}^{137}_{55}\text{Cs}$ in free state show the effect of the electrolytes on MCT where ${}^{137}_{55}\text{Cs}$ nuclei are adsorbed and their decay characteristics are drastically influenced by the density of the trapped neutron in samples from our point of view. Thus, the electrolyte seems to have large effect on the adsorption characteristics of ${}^{137}_{55}\text{Cs}$ by MCT.

This fact reminds us the effect of K and Li on the CFP of Ni and Pd discussed by us for long [Kozima 2000 (Sec. 4), 2006 (Sec. 2.2.1.2)].

“It is should be emphasized here that there are preference for combination of a cathode metal (Pd, Ni, Ti, - -), an electrolyte (Li, Na, K, or Rb) and a solvent (D_2O or H_2O) to induce CFP.” [Kozima 2000 (p. 45)].

Now, let us investigate the characteristics of the decay-time shortening of ${}^{137}_{55}\text{Cs}$ in

these systems.

The temporal evolution of the number of a radioactive nuclide with a decay constant τ is described by following equations;

$$N(t) = N(0) \exp(-t/\tau) \quad (3.2a.4)$$

$$dN/dt = - (N(0)/\tau) \exp(-t/\tau) \quad (3.2a.5)$$

On the other hand, decrease of the number of a nucleus ${}^A_Z\text{X}$ due to absorption of thermal neutrons described by Eq. (3.2a.6) and the relation (3.2a.7) assumed in our model [Kozima 1998 (Sec. 11.1), 2006 (Sec. 3.2)];

$${}^A_Z\text{X} + n = {}^A_Z\text{X}^* = {}^{A+1}_Z\text{X} + \text{phonons}. \quad (3.2a.6)$$

$$P = \delta N_X / N_X = 0.35 n_n v_n \sigma_{nX}, \quad (3.2a.7)$$

where n_n is the density of the trapped neutron, v_n is the thermal velocity of the assumed trapped neutron, N_X is the number of the nucleus ${}^A_Z\text{X}$, and σ_{nX} is the absorption cross section of thermal neutrons by the nucleus X by the reaction (3.2a.6) (= 0.113 b for ${}^{137}_{55}\text{Cs}$) assumed to be the same as the thermal neutron absorption cross section in free space. v_n is taken to be 2.2×10^5 cm/s according to our premises of the TNCF model.

If a ${}^{137}_{55}\text{Cs}$ nucleus is adsorbed by the MCT granules to be reacted by the trapped neutron, the reaction (3.2a.6) is written as,

$${}^{137}_{55}\text{Cs} + n = {}^{138}_{55}\text{Cs}^* = {}^{138}_{55}\text{Cs} + \text{phonons}. \quad (3.2a.8)$$

The reaction occurs with a probability P in a unit time interval for a nucleus ${}^{137}_{55}\text{Cs}$ as expressed in Eq. (3.2a.7):

$$P = \delta N_{Cs} / N_{Cs} = 0.35 n_n v_n \sigma_{nCs}. \quad (3.2a.9)$$

Let us determine the density n_n of the TNCF model assuming that the observed decay-time shortenings of ${}^{137}_{55}\text{Cs}$ in electrolytic liquids depicted in Fig. 2.1 are the results of the neutron absorption described by Eq. (3.2a.8).

For an example of calculation, we take up the case of ${}^{137}_{55}\text{Cs}$ in an electrolytic liquid with MCT + CaCO_3 , where observed the decay time $\tau^* = 310$ d. Using Eq. (3.2a.5), we obtain the relative number of decayed nucleus in a unit time (1 day for instance) as

$$\begin{aligned} \delta N/N &= - (1/\tau^*) \exp(-t/\tau^*) \\ &= - 1/(310 \times 8.64 \times 10^4) = - 1/2.68 \times 10^7 \\ &= 3.73 \times 10^{-8}. \end{aligned} \quad (3.2a.10)$$

In this calculation, we notice that the exponential factor $\exp(-t/\tau^*) \approx 1$ and does not essentially contribute in the final result.

On the other hand, the equation (3.2a.9) gives n_n through the relative number of transmuted ${}^{137}_{55}\text{Cs}$ nuclei $\delta N/N$ as;

$$\begin{aligned} n_n &= (\delta N/N)/(0.35 \times 2.2 \times 10^5 \times 0.113 \times 10^{-24}) \times 1 \text{ (s)} \\ &= (\delta N/N)/(0.35 \times 2.2 \times 0.113 \times 10^{-19}) \end{aligned}$$

$$= 1.15 \times 10^{19} (\delta N/N) \quad (3.2a.11)$$

Using the value of $\delta N/N$ given in Eq. (3.2a.10), we obtain the value of n_n in this case as

$$n_n = 3.73 \times 10^{-8} / 8.70 \times 10^{-19} = 4.29 \times 10^{11} \text{ cm}^{-3} \quad (3.2a.12)$$

If the number of $^{137}_{55}\text{Cs}$ adsorbed by MCT granules and that not adsorbed are in the ratio $x : (1 - x)$, the calculation should be generalized to take into this fact. In the short time (e.g. 1 day) we are interested in, the number N_0 of $^{137}_{55}\text{Cs}$ nuclei not adsorbed and therefore not influenced by the trapped neutron keeps its number $(1 - x)N_0$ almost the same as before (for the very long decay time of $\tau_0 = 30.1$ y):

$$\delta N/N|_1 = 0. \quad (3.2a.13)$$

On the other hand, the nuclei adsorbed by MCT granules will suffer the action of the trapped neutron and its number xN_0 changes according to the equation (3.2a.9):

$$\delta N/N|_2 = 0.35 n_n v_n \sigma_{nM}, \quad (3.2a.14)$$

Therefore, we have the change δN_0 of the number N_0 of $^{137}_{55}\text{Cs}$ nuclei after the time interval t ($= 1$ day) given by $\delta N|_1$ due to the decay process (3.2a.5) with $\tau = 30.1$ y and by $\delta N|_2$ due to the neutron trapping (3.2a.9). Using the relations (3.2a.13) and (3.2a.14), we obtain finally the expression for $\delta N_0 / N_0$ as given in Eq. (3.2a.16):

$$\delta N_0 = \delta N|_1 + \delta N|_2 = \delta(1 - x)N_0|_1 + \delta xN_0|_2 \quad (3.2a.15)$$

$$\delta N_0 / N_0 = x(\delta N_0|_2 / N_0) = x(0.35 n_n v_n \sigma_{nM}) \quad (3.2a.16)$$

Substituting the values $v_n = 2.2 \times 10^5$ cm/s and $\sigma_{nM} = 0.113$ b, we obtain following equation:

$$\begin{aligned} \delta N_0 / N_0 &= x n_n (0.35 \times 2.2 \times 10^5 \times 0.113 \times 10^{-24}) \\ &= 8.7 \times 10^{-21} x n_n \end{aligned} \quad (3.2a.17)$$

Therefore, the value n_n in this case is expressed as

$$n_n = 1.15 \times 10^{19} (\delta N/N) x^{-1} (\text{cm}^{-3}). \quad (3.2a.18)$$

If $x = 1$, i.e. all the $^{137}_{55}\text{Cs}$ nuclei are adsorbed by MCT granules and influenced by the trapped neutron by Eq. (3.2a.8), $\delta N/N = 3.73 \times 10^{-8}$ (3.2a.10) gives the same value given in (3.2a.12);

$$\begin{aligned} n_n &= 1.15 \times 10^{19} (\delta N/N) x^{-1} \\ &= 4.29 \times 10^{11} (\text{cm}^{-3}). \end{aligned} \quad (3.2a.19)$$

This value is compared with the values $10^7 - 10^{12} \text{ cm}^{-3}$ obtained in inorganic CF materials given in our previous books [kozima1998 (Tables 11.2 and 11.3), 2006 (Tables 2.2 and 2.3)].

As the Eq. (3.2a.5) (or Eq. (3.2a.10)) shows that the decrease of the number of radioactive nuclei is proportional to the decay time τ^* inversely and it is also proportional to x and n_n as shown by Eq. (3.2a.16) (where x is the ratio of adsorbed nuclei). The differences of τ^* observed in different electrolytic liquids are explained as

follows.

If the density of trapped neutrons n_n is not influenced by the kind of electrolyte in the liquid, the difference of τ^* depend only on the value of x which may depend on the electrolyte. The values of $\tau^* = 310$ d, 380 d, 480 d, 10 y in the liquid with CaCO_3 , non, NaCl, KCl, respectively, show that the ratios x in these electrolytic liquids are given by 1, 0.8, 0.6, 8.5×10^{-3} , respectively taking the case of CaCO_3 as $x = 1$.

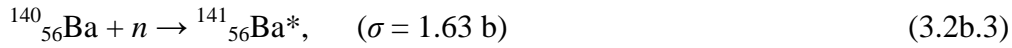
This result may show the aqueous solution of MCT granules is very effective to adsorb $^{137}_{55}\text{Cs}$ nucleus (and change the value of x) and addition of CaCO_3 works positively but that of NaCl and KCl negatively to the adsorption, if our interpretation by the TNCF model of the decay-time shortening in the electrolytic liquids is right.

3.2b $^{140}_{56}\text{Ba}$ and $^{140}_{57}\text{La}$

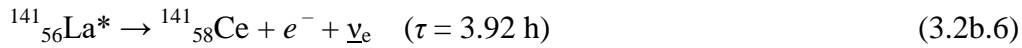
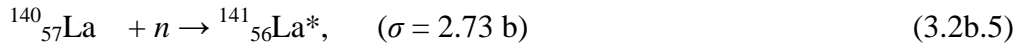
Similarly, we can analyze the cases of $^{140}_{56}\text{Ba}$ and $^{140}_{57}\text{La}$ shown in Fig. 2.2. The decays of these nuclides are described by the following formulae:



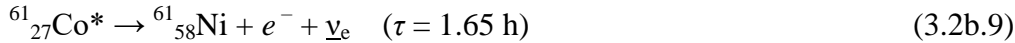
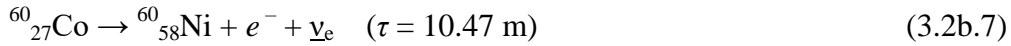
The decay-time shortenings of these nuclides are explained by the absorption of a neutron by $^{140}_{56}\text{Ba}$ and $^{140}_{57}\text{La}$ followed by the beta-decay of the intermediate nuclei as shown below:



and



On the other hand, the decay of $^{60}_{27}\text{Co}$ is not influenced measurably by the existence and absorption of the trapped neutrons as shown by following equations:



Thus, the experimental data for $^{140}_{56}\text{Ba}$, $^{140}_{57}\text{La}$ and $^{60}_{27}\text{Co}$ shown in Fig. 2.2 is consistently explained by the TNCF model.

4. Conclusion

In this paper, we have given our explanation on the nuclear transmutations observed in biological bodies (biotransmutation) as a system composed of carbon and hydrogen. The other two CF materials characterized by carbon and hydrogen, hydrogen graphite

[Kozima 2015 (7)] and XLPE [Kozima 2010, 2016b], had been investigated in other papers using the TNCF model as in this system [Kozima 2015 (8), 2016b].

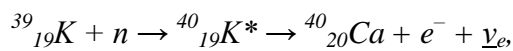
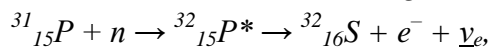
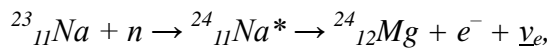
The biotransmutation taken up in this paper is the most difficult problem to understand from physical point of view due to the complex nature of the material where occurs the phenomenon. When we took up the biotransmutation before [Kozima 1996, 1998 (Section 10.1)], the experimental data were just qualitative combining the initial condition characterized by plants (e.g. watercress) or animals (e.g. chicken) and the final results characterized by increases of some elements (e.g. CaO or CaCO₃).

The situation drastically changed mainly by the efforts performed by Vysotskii and his collaborators to identify the elemental changes in rather quantitatively specified materials such biological cultures as *Bacillus subtilis* GSY 228, *Escherichia coli* K-1, *Deinococcus radiodurans* M-1 as well as the yeast culture *Saccharomyces cerevisiae* T-8. Then, we could explain the experimental data of ⁵⁷₂₆Fe production and the decay time shortening of ¹³⁷₅₅Cs, ¹⁴⁰₅₆Ba and ¹⁴⁰₅₇La as presented in the Section 3.1 and 3.2.

We can recite our sentences proclaiming a possibility of biotransmutation to emphasize the weight of the scientific fact even if no framework is absent at the time [Kozima 1998];

“From our point of view, on which the excess heat generation and the nuclear transmutation in electrolytic and gas-loading systems are explained by nuclear reactions in them catalyzed by thermal neutrons, the biotransmutation described in the book and cited above should also be explained as follows.

A body of plants or animals is made of cells with regularity and fundamental elements of the cell are hydrogen (H), oxygen (O) and carbon (C). The ambient thermal neutron, which is plenty on the earth everywhere⁶⁹, can be trapped in the body of a living being by a structure with regularity, i.e. the layer structure of MgATP explained in the Kushi's sentence cited above. The trapped neutron can reacts with an element in the body. Such nuclear transmutation as Na → Mg, P → S, K → Ca and Mn → Fe are easily explained by nuclear reactions where occur a neutron capture and a successive beta decay as follows:



where $\underline{\nu}_e$ is the electron neutrino.” [Kozima 1998 (Section 10.1)]

The variety in the structures and properties of bacteria is very diverse and our explanation on the biotransmutation has been only qualitative. It is, however, possible to

say that the investigation given above in this paper is a first step to understand the mechanism of biotransmutation and may suffice as a corner stone for the science of biotransmutation, an important part of the CFP, with vast possibility of application, especially in the remediation of hazardous nuclear waste with long-lasting radioactivity. It should be mentioned a word on the relation of the TNCF model used to explain the biotransmutations and decay-time shortening in microbial cultures to the “Coherent Correlated States of Interacting Particles” used by Vysotskii et al. [Vysotskii 2015a]. In the bases of the TNCF model, there are several many-body effects working to form the CF-matter as discussed before [Kozima 2014a, 2016]. Detailed investigation of the basis of the “Coherent Correlated States of Interacting Particles” will reveal a close relation of the coherent correlated states to the basis of the TNCF model.

Acknowledgement

The author would like to express his sincere thanks to Dr. V.I. Vysotskii for his kindness to make him easy access to his work, for his information on the molecular structure of the *Escherichia coli* ribosome and also for useful discussions during this work.

Appendix 1: Structures of Bacteria and Microbial Cultures

Perhaps the most obvious structural characteristic of bacteria is (with some exceptions) their small size. For example, *Escherichia coli* cells, an "average" sized bacterium, are about 2 μm long and 0.5 μm in diameter, with a cell volume of 0.6 - 0.7 μm^3 . Small size is extremely important because it allows for a large surface area-to-volume ratio which allows for rapid uptake and intracellular distribution of nutrients and excretion of wastes.

However, the molecular structure of bacteria is very interesting from our point of view in terms of the regular arrangement facilitating interaction with thermal neutrons similar to the XLPE [Kozima 2016b] and also to the transition-metal hydrides introduced in the beginning of this paper. The molecular structure of bacteria, however, is extremely diverse; there are varieties of component structure even if the essential components are common throughout the all bacteria.

To show the general idea of the molecular structure of bacteria, we show first the cell structure of a gram positive bacterium in Fig. A1 and the structure of peptidoglycan, a polymer consisting of sugars and amino acids that forms a mesh-like layer outside the plasma membrane of most bacteria, forming the cell wall, is shown in Fig. A2

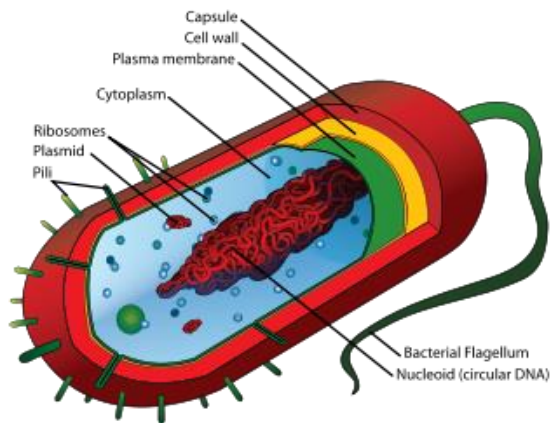


Fig. A1 Cell structure of a gram positive bacterium (after Wikipedia).

Peptidoglycan is made up of a polysaccharide backbone consisting of alternating N-Acetylmuramic acid (NAM) and N-acetylglucosamine (NAG) residues in equal amounts.

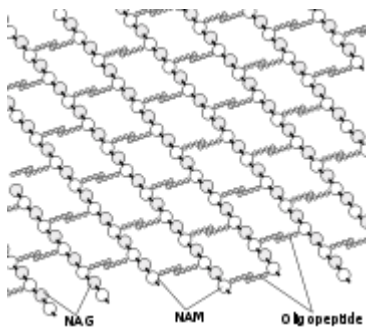


Fig. A2 The structure of peptidoglycan (after Wikipedia).

To understand the periods of molecular structures of bacteria appropriate for the interaction with thermal neutrons, we show the dimension of components of hydrocarbons, ethane, ethylene and benzene, composing the bacteria in Figs. A3 – A5.

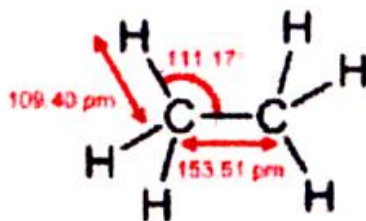


Fig. A3 Ethane molecule

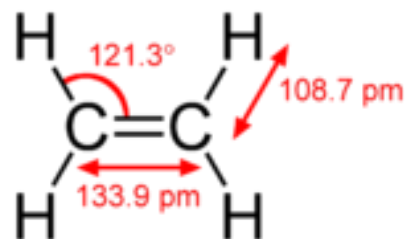


Fig. A4 Ethylene molecule

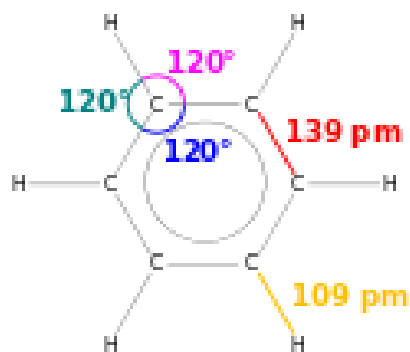


Fig. A5 Benzene molecule

The distances from 108.7 to 139 pm between nuclei in the hydrocarbon molecules given above are compared with the wave length 180 pm of a thermal neutron shown in Section 1.1. This fact shows possibility of interaction of thermal and epithermal neutrons with bacteria resulting in the CFP in biological systems.

The molecular structures of bacteria are, of course, very complicated from one bacterium to another. So, we have to satisfy ourselves only by giving some data of molecular structure of bacteria for a general idea to apply our TNCF model to the biotransmutation (nuclear transmutations in biological system, especially in bacteria).

There are two main types of bacterial cell walls, those of gram-positive bacteria (shown in Fig. A1) and those of gram-negative bacteria as shown in Fig. A6. Gram-positive cell walls are thick and the peptidoglycan (also known as murein) layer constitutes almost 95% of the cell wall in some gram-positive bacteria and as little as 5 – 10% of the cell wall in gram-negative bacteria.

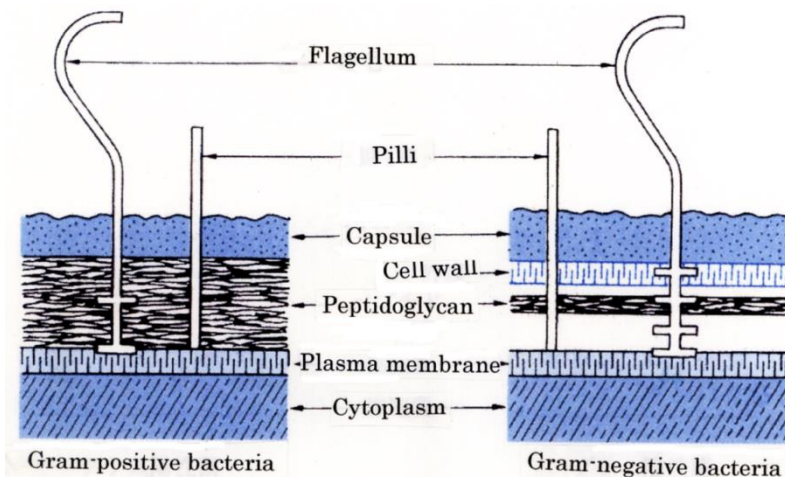


Fig. A6 Structures of cell walls in gram-positive and gram-negative bacteria (after [Ohno 2008]).

The matrix substances in the walls of gram-positive bacteria may be polysaccharides or teichoic acids. These acids are polymers of ribitol phosphate or glycerol phosphate and only located on the surface of many gram-positive bacteria.

Gram-negative cell walls are thin and unlike the gram-positive cell walls, they contain a thin peptidoglycan layer adjacent to the cytoplasmic membrane.

An S-layer (surface layer) is a cell surface protein layer found in many different bacteria and in some archaea, where it serves as the cell wall. All S-layers are made up of a two-dimensional array of proteins and have a crystalline appearance, the symmetry of which differs between species. The exact function of S-layers is unknown, but it has been suggested that they act as a partial permeability barrier for large substrates.

The cell wall has regular array of molecules as shown in Fig. A7 for the case of *Staphylococcus*.

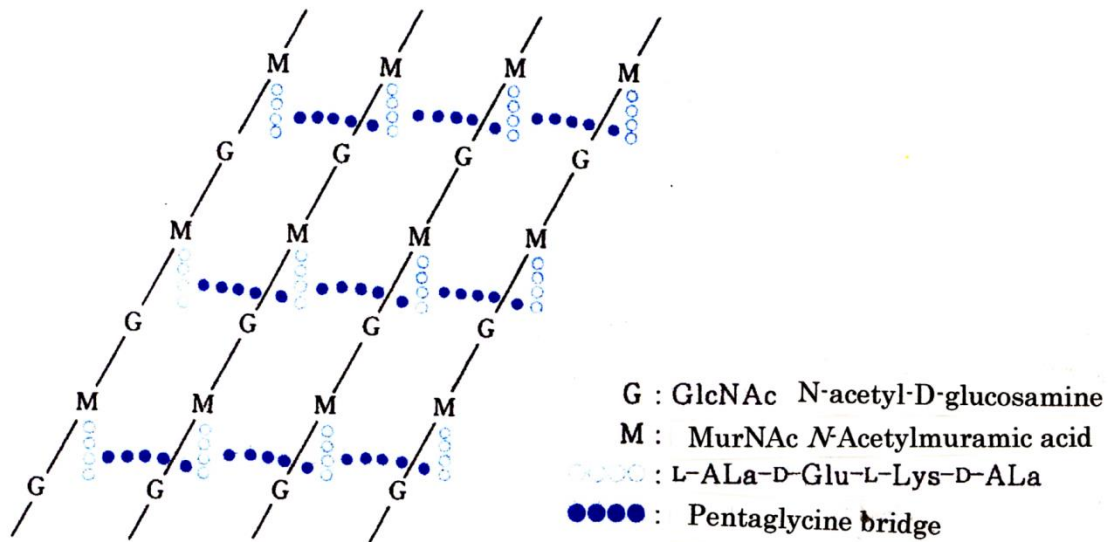
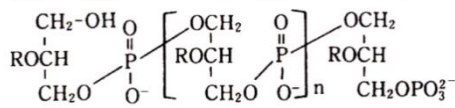


Fig. A7 Structure of the cell wall in *Staphylococcus* (after [Ohno 2008])

Another example of molecular array in bacteria is shown in Fig. A8 for the teichoic acid found within the cell wall of Gram-positive bacteria and appears to extend to the surface of the peptidoglycan layer.

(1) Standard glycerol teichoic acid (Membrane teichoic acid)



(2) Standard ribitol teichoic acid (Cell wall teichoic acid)

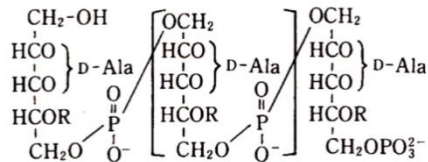


Fig. A8 Molecular structures of teichoic acids; (1) Membrane teichoic acid and (2) Cell wall teichoic acid (after [Ohno 2008]).

Further, the molecular structures of lipopolysaccharide and plasma membrane are shown in Fig. A9 and Fig. A10, respectively.

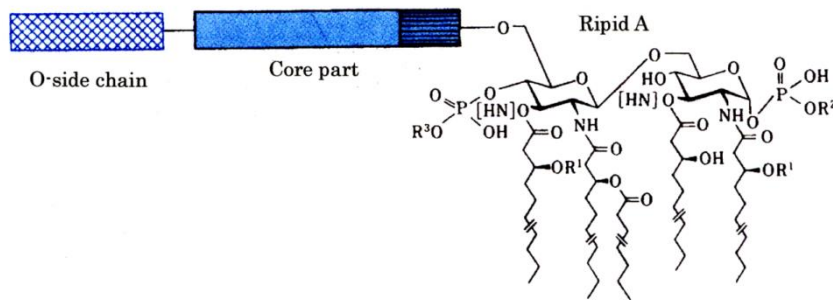


Fig. A9 Molecular structure of lipopolysaccharide (after [Ohno 2008])

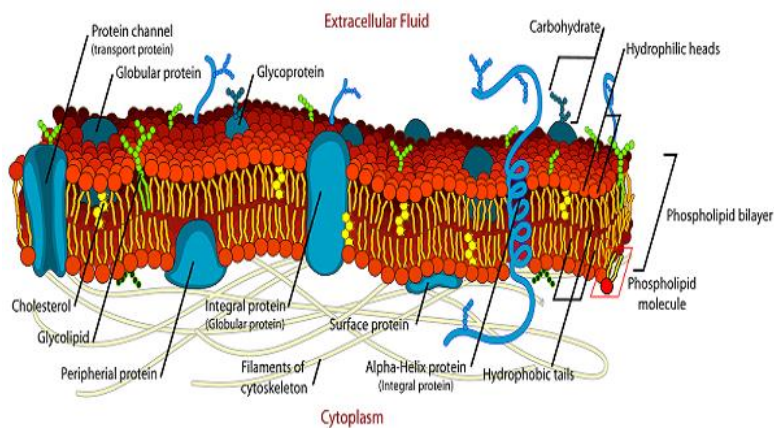


Fig. A10 Structure of plasma membrane

(<http://study.com/academy/lesson/plasma-membrane-of-a-cell-definition-function-structure.html>)

The structure of plasma membrane (cf. Fig. A10) in the bacteria reminds us the structure of XLPE where observed various NTs [Kumazawa 2005], which are explained by the TNCF model [Kozima 2010].

These differences in the structure of molecules in bacteria shown above with several examples (especially in Fig. A6) may have close relation to the characteristics of the biotransmutation induced by a bacterium and useful for their applications.

We can show the molecular structure of the *Escherichia coli* ribosome in Fig. A11 used in the experiments by Vysotskii et al. (e.g. [Vysotskii 2009a]).

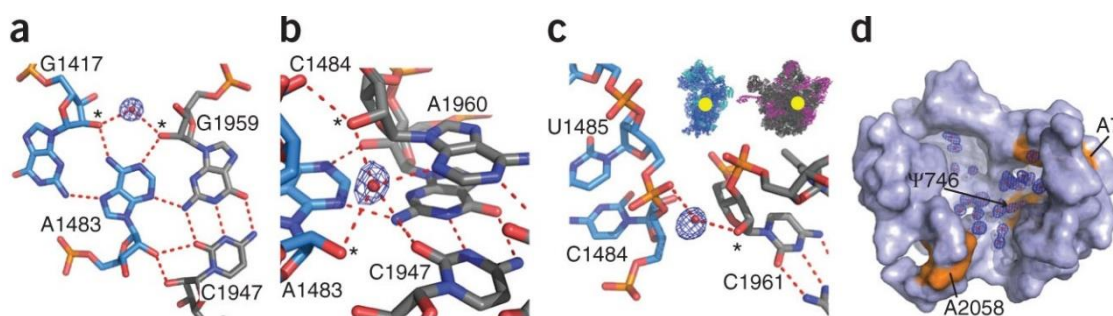


Fig. A11 *Escherichia coli* ribosome [Noeske 2015]

Appendix 2: Microbial Catalyst-Transmutator (MCT) used by Vysotskii et al. [Vysotskii 2009a]

The words MCT (microbial catalyst-transmutator) is used by Vysotskii et al. to express the microbe syntrophin associations used by them as explained in their sentences as cited below from their papers [Vysotskii 2009a, 2013].

“The base of used microbial catalyst-transmutator (MCT) compound is microbe syntrophin associations of thousands different microorganism kinds that are in the state of complete symbiosis. These microorganisms appertain to different physiological groups that represent practically the whole variety of the microbe metabolism and relevantly all kinds of microbe accumulation mechanisms. The state of complete symbiosis of the syntrophin associations results on the possibility of maximal adaptation of the micro-organisms’ association to any external conditions change.

These cultures are in a state of natural complete symbiosis and grow as a total correlated multisystem. There are a lot of different types of intraspecific and interspecific stimulated and symbiotic connections between different cultures in the volume of syntrophin associations. This correlated microbiological multisystem

adequately reacts to modifications of exterior requirements, to composition of nutrient medium and to biochemical properties of a system because of metabolic, growth and transmutation processes. The spectrum of their functional characteristics is very wide. We believe that it should be expected that this would lead to high efficiency for stimulating transmutation processes. This model is presented in symbolic form on Fig. 3.15.” [Vysotskii 2009a] (Fig. 3.15 of this paper is cited below as Fig. A12).

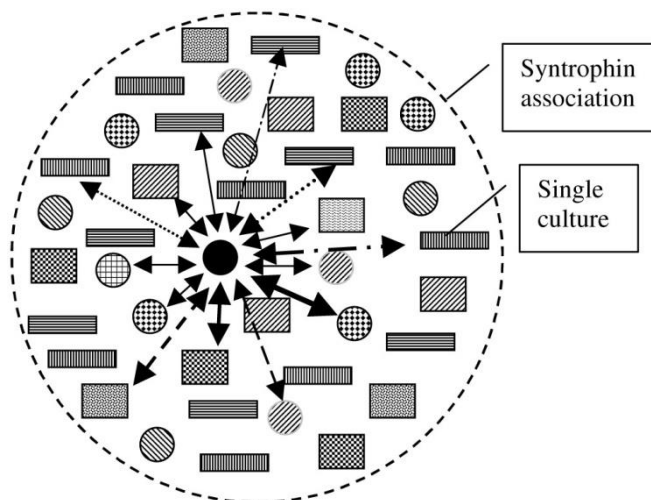


Fig. A12 Symbolic scheme of different types of intraspecific and interspecific connections between arbitrary selected culture and different cultures in the volume of syntrophin association. The same connections are related to each culture.“ [Vysotskii 2009a (p. 53, Fig. 3.15)]

“The base of MCT (“microbial catalyst-transmutator”) compound that was used is the microbe syntrophin associations of thousands different microorganism kinds that are in the state of complete symbiosis (Vysotskii et al., 2003b; Vysotskii et al., 2008; Vysotskii and Kornilova, 2009). These microorganisms appertain to different physiological groups that represent practically the whole variety of the microbe metabolism and relevantly all kinds of microbe accumulation mechanisms. We postulate that the state of complete symbiosis of the syntrophin associations results from the possibility of maximal adaptation of the microorganisms’association in response to changes in any external condition. These cultures are in a state of natural complete symbiosis and grow as a total correlated multisystem. There are a lot of different types of intraspecific and interspecific stimulated and symbiotic connections between different cultures in the volume of syntrophin associations. This microbiological multisystem adequately reacts to modifications of exterior requirements, to composition of nutrient medium and to

biochemical properties of a system because of metabolic, growth and transmutation processes.

The MCT compound involves special granules that include:

- *Concentrated biomass of metabolically active microorganisms (microbe syntrophin association);*
- *Organic sources of carbon and energy, phosphorus, nitrogen, etc.*
- *Gluing substances that keep all components in the form of granules stable in water solutions, for a long period of time, subjected to many, possibly any, external conditions.” [Vysotskii 2013]*

“The MCT represents special granules that include: concentrated biomass of metabolically active microorganisms, sources of carbon and energy, phosphorus, nitrogen, etc., and gluing substances which keep all components in the way of granules stable in water solutions for a long period of time at any external conditions. The base of the MCT are microbe syntrophin associations that contain many thousands kinds of different microorganisms that are in the state of complete symbiosis. These microorganisms appertain to different physiological groups that represent practically whole variety of the microbe metabolism and relevantly all kinds of microbe accumulation mechanisms.” (Vysotskii et al. “Experimental Study of Accelerated Deactivation of High-activity Reactor Water in Growing Microbiological Cultures”).

References

[Komaki 1993] H. Komaki, “Observations on the Biological Cold Fusion or the Biological Transmutation of Elements,” *Proc. ICCF3*, pp. 555 – 558 (1993), ISBN 4-946443-12-6.

[Kozima 1994] H. Kozima, “Trapped Neutron Catalyzed Fusion of Deuterons and Protons in Inhomogeneous Solids,” *Trans. Fusion Technol.* **26**, 508 – 515 (1994). ISSN 0748-1896.

[Kozima 1996] H. Kozima, K. Hiroe, M. Nomura and M. Ohta, “Elemental Transmutations in Biological and Chemical Systems,” *Cold Fusion*, **16**, 30 – 32 (1996), ISSN 1074-5610.

[Kozima 1998] H. Kozima, *Discovery of the Cold Fusion Phenomenon* (Ohtake Shuppan Inc., 1998), ISBN 4-87186-044-2. (Section 10.1 Biotransmutation)

[Kozima 2000] H. Kozima, “Electroanalytical Chemistry in Cold Fusion Phenomenon,” in *Recent Research Developments in Electroanalytical Chemistry*, ed. S.G. Pandalai, Transworld Research Network, 2000, ISBN 81-86486-94-8.

[Kozima 2005] H. Kozima, “CF-Matter and the Cold Fusion Phenomenon,” *Proc. ICCF10*, pp. 919 – 928 (2005), ISBN 981-256-564-7.

[Kozima 2006] H. Kozima, *The Science of the Cold Fusion Phenomenon*, Elsevier Science, 2006, ISBN-10: 0-08-045110-1.

[Kozima 2008] H. Kozima and T. Date, “Nuclear Transmutations in Polyethylene (XLPE) Films and Water Tree Generation in Them,” *Proc. ICCF14* (August 10 – 15, 2008, Washington D.C., U.S.A.) pp. 618 – 622 (2010), ISBN:978-0-578-06694-3. And also *Reports of CFRL (Cold Fusion Research Laboratory)*, **8-2**, pp. 1 – 16 (August, 2008):

<http://www.geocities.jp/hjrfq930/Papers/paperr/paperr.html>

[Kozima 2010] H. Kozima and H. Date, “Nuclear Transmutations in Polyethylene (XLPE) Films and Water Tree Generation in Them,” *Proc. ICCF14* (August 10 – 15, 2008, Washington D.C., U.S.A.) pp. 618 – 622 (2010), ISBN 978-0-578-06694-3. And also *Reports of CFRL (Cold Fusion Research Laboratory)*, **8-2**, pp. 1 – 16 (August, 2008); <http://www.geocities.jp/hjrfq930/Papers/paperr/paperr.html>

[Kozima 2014a] H. Kozima, “The Cold Fusion Phenomenon – What is It?” *Proc. JCF14*, **14-16**, pp. 203 – 230 (2014), ISSN 2187-2260, and posted at JCF website:

<http://jcfirs.org/file/jcf14-proceedings.pdf>. And also *Reports of CFRL 14-4*, 1 – 29 (March, 2014) which is posted at CFRL website:

<http://www.geocities.jp/hjrfq930/Papers/paperr/paperr.html>

[Kozima 2014b] H. Kozima, “Nuclear Transmutations (NTs) in Cold Fusion Phenomenon (CFP) and Nuclear Physics,” *Proc. JCF14:14-15*, pp. 168 - 202 (2014), ISSN 2187-2260; <http://jcfirs.org/file/jcf14-proceedings.pdf>. And also *Reports of CFRL (Cold Fusion Research Laboratory) 14-3*, 1 – 35 (March, 2014):

<http://www.geocities.jp/hjrfq930/Papers/paperr/paperr.html>

[Kozima 2014c] H. Kozima, “Nuclear Transmutation in Actinoid Hydrides and Deuterides,” *Proc. JCF14:14-6*, pp. 77 – 94 (2014), ISSN 2187-2260. And also *Reports of CFRL (Cold Fusion Research Laboratory) 14-2*, 1 – 18 (March, 2014);

<http://www.geocities.jp/hjrfq930/Papers/paperr/paperr.html>

[Kozima 2015] H. Kozima, “The Nuclear Transmutations (NTs) in Carbon-Hydrogen Systems (Hydrogen Graphite, XLPE and Microbial Cultures),” *From the History of Cold Fusion Research*, **8**, pp. 1 – 23 (June 2015):

<http://www.geocities.jp/hjrfq930/Papers/paperf/paperf.html>.

[Kozima 2016a] H. Kozima and K. Kaki, “The Cold Fusion Phenomenon and Neutrons in Solids,” *Proc. JCF16* (to be published), ISSN 2187-2260, and to be posted at JCF website: <http://jcfirs.org/file/jcf14-proceedings.pdf>.

- [Kozima 2016b] H. Kozima, “Nuclear Transmutations in Polyethylene (XLPE) Films and Water Tree Generation in Them (2),” *Proc. JCF16* (to be published), ISSN 2187-2260, and to be posted at JCF website: <http://jcfrs.org/file/jcf14-proceedings.pdf>.
- [Kushi 1994] M. Kushi, *The Philosopher’s Stone*, One Peace World Press, 1994.
- [Noeske 2015] J. Noeske, M.R. Wasserman, D.S. Terry, R.B. Altman, S.C. Blanchard and J.H.D. Cate, “High-resolution Structure of the *Escherichia coli* ribosome,” *nature structural & molecular biology*, advance online publication, doi:10.1038/nsmb.2994, pp. 1 – 7 (2015).
- [Ohno 2008] N. Ohno and M. Sasatsu Ed. *New Microbiology*, 3rd edition, Hirokawa Publishing Co., 2008 (in Japanese), ISBN 978-4-567-52055-3.
- [Storms 2007] E. Storms, *The Science of Low Energy Nuclear Reaction*, World Scientific, 2007, ISBN-10 981-270-620-8.
- [Suess 1956] H.E. Suess and H.C. Urey, “Abundances of the Elements,” *Rev. Mod. Physics* **28**, 53 – 74 (1956).
- [Vysotskii 1996] V.I. Vysotskii, A.A. Kornikova and I.I. Samoylenko, “Experimental Discovery of the Phenomenon of Low-Energy Nuclear Transmutation of Isotopes ($^{55}\text{Mn} \rightarrow ^{57}\text{Fe}$) in Growing Biological Cultures,” *Proc. ICCF6*, pp. 687 – 693 (1996).
- [Vysotskii 2000] V.I. Vysotskii, A.A. Kornikova, I.I. Samoylenko and G.A. Zykov, “Experimental Observation and Study of Controlled Transmutation of Intermediate Mass Isotopes in Growing Biological Cultures,” *Proc. ICCF8*, pp. 135 – 140 (2000).
- [Vysotskii 2009a] V.I. Vysotskii and A.A. Kornilova, *Nuclear Transmutation of Stable and Radioactive Isotopes in Growing Biological Systems*, Pentagon Press, India, 2009.
- [Vysotskii 2009b] V.I. Vysotskii and A.A. Kornilova, “Nuclear Transmutation of Isotopes in Biological Systems (History, Models, Experiments, Perspectives),” *Journal of Scientific Exploration*, **23**, pp. 496-500 (2009)
- [Vysotskii 2013] V.I. Vysotskii and A.A. Kornilova, “Transmutation of Stable Isotopes and Deactivation of Radioactive Waste,” *Annals of Nuclear Energy* **62**, 626–633 (2013).
- [Vysotskii 2015a] V.I. Vysotskii and M.V. Vysotsky, “Coherent Correlated States of Interacting Particles – the Possible Key to Paradoxes and Features of LENR,” *Current Science*, **108**, 524 – 531 (2015).
- [Vysotskii 2015b] V.I. Vysotskii and A.A. Kornilova, “Microbial Transmutation of Cs-137 and LENR in Growing Biological Systems,” *Current Science*, **108**, 636 – 641 (2015). (increasing decay rate of Cs-137 isotope)